J. Condensed Matter Nucl. Sci. 24 (2017) 25–31

Research Article

Fluorescence-based Temperature Sensor for Anomalous Heat from Loaded Palladium Electrodes with Deuterium or Hydrogen

Sangho Bok*, Cherian Mathai, Keshab Gangopadhyay and Shubhra Gangopadhyay†
Department of Electrical Engineering, University of Missouri, Columbia, MO, USA

Orchideh Azizi , Jinghao He, Arik El-Boher, Graham Hubler and Dennis Pease
The Sydney Kimmel Institute for Nuclear Renaissance (SKINR), Department of Physics and Astronomy, University of Missouri, Columbia, MO, USA

Abstract

Anomalous heat generation in palladium-based materials has been studied in various active research groups since M. Fleischmann, and S. Pons demonstrated an anomalous heat in 1989. There have been attempts to explain anomalous heat by deuteron–deuteron nuclear fusion in the Pd lattice while the search for radiation was unsuccessful which indicated that the origin of the excess heat is unknown. Despite the unknown origin of the excess heat, Pd system is in the core of the research for energy production. The excess heat has been demonstrated by using calorimeters that are well characterized. However, these measurements are not able to provide detailed information about a localized heat rather than a heat from a large area. A new method is demonstrated to investigate an excess heat from Pd electrode loaded with deuterium or hydrogen. It is capable of measuring a small amount of heat generated in a localized area with a sub-micrometer resolution by fluorescence imaging with temperature sensitive fluorescence dyes. Considering quantum yield, photostability, and thermal stability, rhodamine 6G (R6G) is selected for temperature sensor along with a polymer, Poly MethylSilsesquioxane (PMSSQ). The thermal quenching of fluorescence resulted in a decreased temperature over time with heat generation. We envisioned that this new method of the temperature measurement provided a novel diagnostic tool for localized excess heat which was not detectable by calorimetry due to intrinsic disability.
 ISSN 2227-3123

Keywords: Anomalous heat, Fluorescence, Temperature sensor

1. Introduction

Since the demonstration of anomalous heat in 1989 by M. Fleischmann, and S. Pons, anomalous heat generation in palladium-based materials has been studied in various active research groups [1]. Different types of electrodes

*Present address: Department of Engineering and Technology, Southern Utah University, Cedar City, UT, USA.
† Corresponding author. E-mail: gangopadhyays@missouri.edu.

 ISSN 2227-3123

have been tried to reproduce the excess heat. A few exemplary electrodes are Palladium (Pd)-Single Walled Carbon Nanotubes (SWCNT), Pd nanoparticles, and other metals like hydrogen loaded nickel [2]. The origin of the anomalous heat is arguably uncertain because numerous attempts to explain anomalous heat by deuteron-deuteron nuclear fusion in the Pd lattice while the search for radiation was unsuccessful. Although the origin of the excess heat is unknown, Pd electrodes are in the core of the research for excess heat. The demonstration of the excess heat utilizes calorimeters that are well characterized with known errors and limitations as well as beneficial strengths [3]. However, these measurements are not able to provide detailed information about a localized heat rather than a heat from a large area.

Temperature (T) is one of the most fundamental parameters in science and daily life. Temperature sensors are commonly used in various fields such as metrology, biology, engineering, climate research, and nanotechnology to name a few in addition to daily life devices like heating and cooling systems, food storage, and production of plants. The important of the temperature sensors are reflected to the market share of about 75% in the world sensor markets [4]. There are different types of temperatures sensors including liquid-filled glass thermometers based on the thermal expansion of materials [5], thermocouples based on the Seebeck effect [6], and optical sensors [7]. Optical temperature sensors have a unique advantage of large-scale temperature measurement with high resolution based on the imaging technique [8]. Among various optical temperature sensors including infrared (IR) thermometers, fluorescence temperature sensor is of our interest because it has a potential of using each fluorophore as a temperature probe.

Fluorescence temperature sensing mechanism have various attractive benefits including the potential of the high resolution temperature monitoring when a single fluorophore acts as a temperature probe. Temperature sensor with fluorescence is almost exclusively based on the fluorophore which can be fluorescent dye molecules, fluorescence nanoparticles or aggregates of fluorophores. The temperature probes can be incorporated in the samples of the study or deposited on its surface in the form of a polymer containing the probes. It has been reported that the measurement can be performed for a single point analysis and the large area by imaging technique [9].

The micro-/nano-scale studies of temperature variation require the use of micro-/nano-size temperature sensors. One of the highlighted studies is nanoparticles such as quantum dots and fluorescence dye molecules [8,9] in combination with spectroscopy or microscopy. To achieve sub-micrometer scale resolution in temperature sensing, the measurement systems need to be capable of measuring such resolution. Recent development on super-resolution microscopy has adequate functionalities of this purpose [10]. However, the super-resolution microscopy is expensive and require special training which leaves a question of practical application in low cost and ease of use. Temperature sensitive fluorescent dyes such as rhodamine 6G (R6G) have drawn great interests due to their real-time temperature measurement capability, large area measurement with high resolution, and ease of incorporation in polymer matrices. The plasmonic grating can significantly enhance the fluorescence intensity by coupling both excitation and emission of fluorophores when satisfying the wave vector matching condition [11,12]. Moreover, it can serve as super-resolution imaging platform to visualize nanostructures [11] to image localized heat generation on the Pd electrodes in sub-micrometer scale.

In this article, we demonstrated a temperature characterization method incorporating R6G/polymer coating matrix on top of the Pd electrodes using a simple epi-fluorescence microscope. We experimentally developed a method for dynamic thermal mapping with this temperature sensitive dyes. First, we prepared Pd electrodes with a temperature sensitive R6G mixed with a polymer matrix, poly methyl silsesquioxane (PMSSQ) on Pd electrodes. Then, we established temperature-fluorescence calibration curve for R6G/PMSSQ systems via fluorescence characteristics by a microscope equipped with a heat stage.

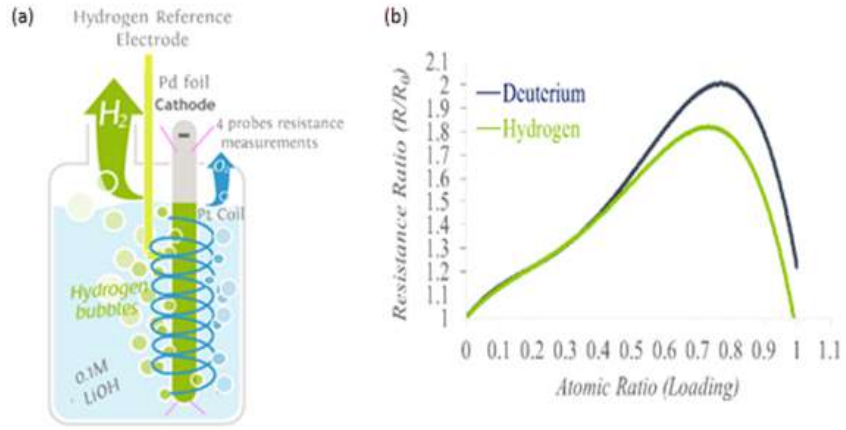

Figure 1. (a) Standard three electrode electrochemical cell; (b) Resistance ratio (R/R_0) vs. loading ratio for the Pd/H and Pd/D systems at 25°C [13].

2. Experiment

2.1. Chemicals and materials

Laser grade R6G was obtained from Exciton (Dayton, OH) and PMSSQ (14% -OH) was purchased from Technelglas (Perrysburg, OH). 200 proof ethanol was purchased from Sigma Aldrich and used as-received. Other analytic grade chemicals such as nitric acid, sulfuric acid, lithium hydroxide were purchased from Sigma Aldrich and used as-received. Deionized (DI) water was used for cleaning and solution preparation.

2.2. Preparation of palladium electrode

Palladium foils of 50 μm thickness were prepared using cold rolling of a 1 mm thick palladium (Holland Moran) followed by thermal annealing at 850°C for 60 min in a protocol to ensure all samples have the same initial conditions. A platinum wire and a standard hydrogen electrode (RHE) were used as a counter and reference electrode, respectively. All potentials are recorded with respect to RHE.

A standard three-electrode electrochemical cell was used to loading hydrogen and deuterium in Pd foils, Fig. 1a. The H(D) loading was determined using in-situ four probe resistance measurements. Figure 1b shows the relation between resistance ratio (R/R_0) versus hydrogen and deuterium atomic ratio in palladium (H/Pd and D/Pd) [13]. The resistance of palladium is expressed as a ratio R/R_0, where R is the resistance at a particular loading and R_0 is the resistance of the unloaded Pd. The working electrode was a Pd foil of 2.8 cm^2 attached to five platinum wires, among which four wires were used for the resistance measurement and one wire for current supply. All experiments were performed at room temperature in 0.1 M LiOH or LiOD solutions. 5 mM Hg_2SO_4 was introduced in increments as an impurity into the 0.1 M LiOH (LiOD) solutions in a standard cell to give a concentration between 40 and 400 ppb to enhance H(D) loading in Pd foils and prevent H(D) deloading after the current was tuned off [14].

2.3. Temperature sensitive dye/polymer coating

R6G/PMSSQ solution was prepared by dissolving PMSSQ and R6G in pure ethanol with a final concentration of 1 wt.% PMSSQ and 10 μM R6G (excitation: 530 nm, emission: 550 nm) followed by 10 min sonication. Loaded Pd

electrodes described previously and unloaded Pd electrodes were spin-coated at 3000 RPM for 30 s with R6G/PMSSQ solution. This method was expected to produce a conformal, 30 nm-thick layer of fluorophore incorporated PMSSQ on top of the Pd electrodes. The addition of this coating was performed immediately after the loaded samples were out of the loading solution to minimize deloading of H(D) from Pd electrodes. The coated Pd electrodes were imaged with an Olympus BX51WI epifluorescence microscope as described in Section 2.4.

2.4. Image acquisition and image analysis

The R6G/PMSSQ coated Pd electrodes were imaged with an Olympus BX51WI epifluorescence microscope equipped an ORCA-flash 2.8 CCD camera, 10/20/40 $\times$ objectives, and illuminated with a fluorescent filter cube. A xenon broadband light source was combined with fluorescent filter cube (an excitation filter (518 nm/20 nm) and a long pass emission filter (541 nm)). The electrode was placed on a pre-cleaned glass slide before the measurement. Same spots of the immobilized electrode were imaged in various times up to several days in different intervals. For analysis, Image J software was utilized. An image taken at 0 min (immediately after the sample was placed under the microscope) was chosen for base fluorescence intensity. Images taken at various time were compared in fluorescence intensity at the same spots.

3. Results and Discussion

Since the first claim from Fleischmann and Pons [1] for an anomalous production of heat obtained during an electrochemical experiment, a great number of experiments has been devised and performed, in order to confirm or disprove the effect. The initial disappointment at lack of experimental reproducibility has by now been compensated to a fair degree by realizing special conditions that are usually difficult to achieve [3]. For example, it is now known that a high D/Pd loading ratio is one such difficult necessary condition and that likely there are others. Thus, we carefully prepared each electrode so that it achieved at least D/Pd $>92\%$ because it was reported that no excess heat was observed from the electrodes that had a D/Pd $<90\%$.

Figure 2 shows the resistance ratio (R/R_0) of Pd as a function of time in electrolysis in a pure 0.1 M LiOD solution and then the effect of additions of Hg_2SO_4 salt into the electrolyte at different time intervals after the ß phase was formed. The results show that an addition of few ppb level of mercury salt at low current densities results in a decrease of the R/R_0 (increase in atomic ratio D/Pd) in a short time. Also, the results show that it is possible to maintain a high loading for more than few weeks by keeping adding mercury salt during electrolysis.

Deuterium loading ratio in a Pd foil was also measured ex-situ using a Rigaku X-ray diffractometer. After a Pd foil was loaded to R/R_0 =1.68 (D/Pd~92–95%) in a solution in the presence of Hg_2SO_4, the sample was immediately taken out from an electrochemical cell for the X-ray diffraction (XRD) measurement. Lattice parameter calculated by XRD is about $\sim$4.08 AU which corresponds to the atomic ratio of D/Pd $\sim$100% within the depth of a few microns (X-ray penetration depth) in the Pd foil. The XRD measurement showed no significant deloading occurred after the sample was exposed in air for more than 1 h.

The temperature mapping for loaded Pd was conducted without laser/RF excitation to simplify the experimental procedure. Therefore, the temperature change resulted from a slow monoatomic deloading deuterium or hydrogen from the Pd lattice and recombination into molecules of D_2/H_2. This exothermic process causes thermal quenching of fluorescence. There are reports on fluorescence thermal quenching processes that are utilized as temperature probes. There are multiple pathways for fluorescence dyes to lose the fluorescence such as oxidation, degradation, quenching, and photobleaching. In the presented experimental condition, oxidation and degradation are not significant comparing to photobleaching which is a major concern for fluorescence dyes [15]. Due to the photobleaching, it is critical to consider the decay of fluorescence over the measurement time as the thermal quenching may be screened. To prevent

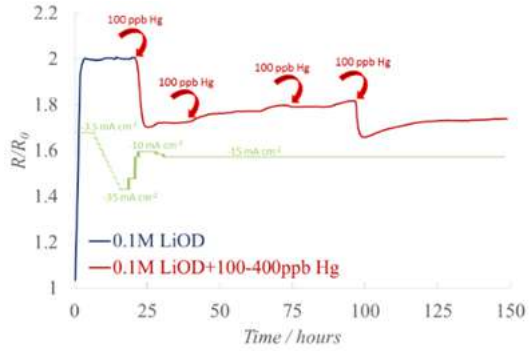

Figure 2. Deuterium loading (R/R_0) into Pd in 0.1 M LiOD electrolyte. 100–400 ppb Hg_2SO_4 was added to the electrolyte after a-phase was fully transformed to ß-phase and a steady state loading ratio was reached.

the misleading effect of photobleaching, R6G/PMMSQ on unloaded Pd electrodes were examined Unloaded Pd electrodes did not have any exothermic process and therefore, fluorescence decay observed was due to the photobleaching by multiple exposure of the R6G/PMSSQ coating on Pd at the same measurement spots. This calibrated photobleaching data were utilized to compensate the measurement of the loaded Pd electrodes. Once the exothermic process is finished, either the fluorescence recovers or the fluorescence dyes decompose (>250°C) remaining in a low fluorescence. Experimental results undoubtedly showed localized temperature changes after the images were subtracted from the reference fluorescence image (measured at 0 min). Figure 3(a) is obtained by subtracting a fluorescence image at 48 h from a fluorescence image at 0 min. If there is heat generated at specific regions, quenching suppresses fluorescence. By subtracting it from unquenched image, we obtain bright spots in Fig. 3(a) as heat generated regions and dark spots as no heat generation. Figure 3(a) presented three different regions (red circles) with corresponding temperature changes (Fig. 3(b)). The temperature increased over time while region three had fluorescence recovery (from 19 to 48 h) resulting in temperature reduction after subtracting the effect of calibrated photobleaching.

The temperature changes were consistently observed from other loaded Pd electrodes as summarized in Table 1. Although there was no correlation of the behavior between grain boundary and grain in terms of temperature variation,

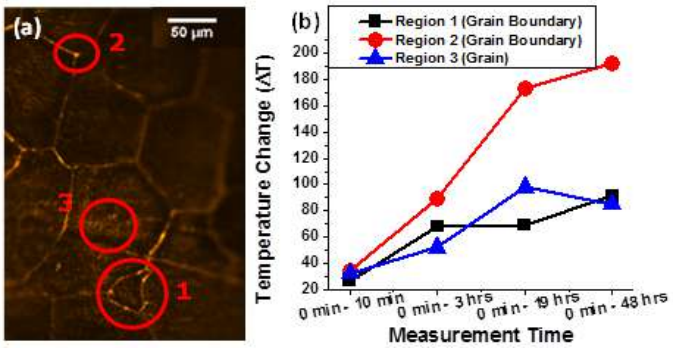

Figure 3. (a) Fluorescence image of a loaded Pd coated with a 30nm R6G/PMSSQ. The image was captured in an epi-fluorescence microscope (10×) with an excitation filter (518 nm/20 nm)/long pass emission filter (541 nm). (b) Temperature changes in grain boundaries (regions 1 and 2) and on grain (region 3).

Table 1. Fluorescence quenching for loaded Pd electrode.

Subtracted mages	Intensity difference (thermal quenching)	
	Grain boundary (AU)	Grain (AU)
0 min–10 min	433	839
0 min–60 min	1428	960
0 min–2 h	1715	1107
0 min–3 h	1925	1531
0 min–22 h	2391	1848

it was evident that most of area showed temperature increase (i.e. fluorescence decrease). The subtraction of fluorescence intensity (e.g. 0 min image – 10 min image) was 433 and 839 AU on grain boundary and grain, respectively. After 22 h, the subtraction became 2391 and 1848 AU on grain boundary and grain, respectively. This means that the electrode generated heat increasingly over time. In 22 h, the photobleaching was estimated to have 600 AU. After considering a photobleaching calibration curve, R6G thermal quenching fluorescence intensity was obtained as below [8]:

$$I = [-0.41\%(T - T_0) + 1]I_0, \quad T_0 = 27^{\circ}\mathrm{C}. \tag{1}$$

From Eq. (1), the temperature changes (ΔT) were calculated for the grain (1848 AU at 22 h) to be 148°C.

In the current study, up to 40× objective was utilized because higher objectives are available for water or oil immersion. The 40× objective allowed us to observe the Pd electrode in air without damaging the samples with other media. Based on the optical arrangement and the objective, the image had a resolution of 300 nm ×300 nm pixel as shown in Fig. 4. The pixel was a potentially a temperature probe which included multiple fluorophores. Considering the recent advancement in *super-resolution* microscopy, it is expected to have much higher resolution (∼20 nm) [8].

4. Conclusion

We have demonstrated a new method as a temperature probe to investigate an anomalous heat from Pd electrode. Current experimental setups utilizing calorimetry are well calibrated for measurement of bulk temperature changes in the experimental cell. The fluorescence based temperature probe is capable of identifying and mapping a very local temperature changes close to 300 nm with a potential for 20 nm combining with the super-resolution analysis. We envisioned that this new method provided a novel diagnostic tool for localized heat which was not detectable by

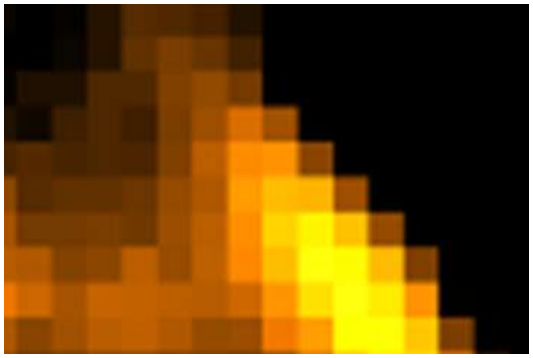

Figure 4. Zoom-in of the original image showed pixels. Each pixel was 300 nm ×300 nm which depended on magnification of objective.

calorimetry. Further study includes that excitation of the loaded Pd will be performed with various sources such as lasers and RF to investigate excess heat.

Acknowledgements

The study is supported by the Sidney Kimmel Foundation, USA.

References

[1] M. Fleischmann, S. Pons and M. Hawkins, *J. Electroanal. Chem*. 261 (1989) 301 and errata in Vol. 263.
[2] O. Azizi, A. El-Boher, J. H. He, G. K. Hubler, D. Pease, W. Isaacson, V. Violante and S. Gangopadhyay, *Current Sci.* **108** (4) (2015) 565–573.
[3] A. Kitamura, T. Nohmi, Y. Sasaki, A. Takahashi, R. Seto and Y. Fujita, *Phys. Lett.* A **373** (2009) 3109–3112.
[4] P.R.N. Childs, J.R. Greenwood and C.A. Long, *Rev. Sci. Instrum.* **71** (2000) 2959–2978.
[5] L. Michalski, K. Eckersdorf, J. Kucharski and J. McGhee, *Temperature Measurement*, Wiley, Chichester, UK, 2001.
[6] S. Maekawa, *Physics of Transition Metal Oxides*, Springer, 2004.
[7] G. Beheim, Integrated optics, *Microstructures and Sensors* (1995) 285–313.
[8] B. Chen, H. Zheng, J. Yoon, S. Bok, C. Mathai, K. Gangopadhyay, S. Gangopadhyay M.R. Maschmann, Sensors, *IEEE*, 2016.
[9] X. Wang, O.S. Wolfbeis and R.J. Meier, *Chem. Soc. Rev.* **42** (2013) 7834.
[10] A. Wood, B. Chen, C. Mathai, S. Bok, S. Grant, K. Gangopadhyay, P.V. Cornish and S. Gangopadhyay, *Microscopy Today* 25 (1) (2017) 42–47.
[11] B. Chen, A. Wood, A. Pathak, J. Mathai, S. Bok, H. Zheng, S. Hamm, S. Basuray, S. Grant, K. Gangopadhyay, P. V. Cornish and S. Gangopadhyay, *Nanoscale* **8** (2016) 12189–12201.
[12] A. Wood, B. Chen, S. Pathan, S. Bok, C.J. Mathai, K. Gangopadhyay, S.A. Grant and S. Gangopadhyay, *RSC Advances* **5**(96) (2015) 78534–78544.
[13] W. Zhang, Z. Zhang and Z.L. Zhang, *J. Electroanal. Chem*. **528** (2002) 1.
[14] F.L. Tanzella, S. Crouch-Baker, A. McKeown and M.C.H. McKubre, *ICCF6*, Japan, 1996.
[15] S. Bok, V. Korampally, L. Polo-Parada, V. Mamidi, G.A. Baker, K. Gangopadhyay, W.R. Folk, P.K. Dasgupta and S. Gangopadhyay, *Nanotechnology* **23**(17) (2012) 175601.